AMER. ZOOL., 41:1036–1048 (2001)

Mechanism of Postinhibitory Rebound in Molluscan Neurons[1]

BRADLEY R. JONES* AND STUART H. THOMPSON[2,†]

*Pacific Biomedical Research Center, 1993 East-West Road, University of Hawaii, Honolulu, Hawaii 96822
†Hopkins Marine Station, Stanford University, Pacific Grove, California 93950

SYNOPSIS. Postinhibitory rebound (PIR) is an intrinsic property of many neurons but the underlying mechanism is not well understood. We studied PIR and its relationship to spike adaptation in B-cells isolated from the buccal ganglia of *Aplysia.* These neurons exhibit PIR following inhibitory synaptic input and following direct membrane hyperpolarization. Hyperpolarizing and depolarizing voltage clamp pulses from the resting potential evoke slow changes in membrane current that persist in the form of tail currents following the pulses. A subtraction method was used to isolate slow tail currents for study. Current-voltage measurements indicate that slow outward tail currents following depolarizing pulses result from increases in membrane conductance, while inward tail currents following hyperpolarizations to −50 and −60 mV result from conductance decreases. The reversal potential of both outward and inward tail current is between −60 and −70 mV. Tail currents activated by pulses more positive than −60 mV are sensitive to the external K^+ concentration and blocked by injection of Cs^+ and TEA. When Ca^{2+} influx is prevented by bathing cells in Ca^{2+} free saline or by adding Co^{2+} or Ni^{2+}, the tail currents are reduced but a significant fraction of the current is insensitive to these treatments. More negative conditioning pulses activate a second component of inward tail current that is weakly sensitive to K^+ but more strongly effected by substitution of N-methyl glucamine or Li^+ for external Na^+. We conclude that both PIR and adaptation result from slow changes in a voltage dependent, non-inactivating K^+ conductance that is active at voltages near the resting potential and is not tightly coupled to Ca^{2+} influx. In addition, a second inward current is activated by large hyperpolarizing pulses that results from an increase in Na^+ and K^+ conductance. This second process is likely to contribute to PIR under particular circumstances.

INTRODUCTION

The term *postinhibitory rebound* (PIR) refers to a period of increased neuronal excitability following the cessation of inhibition. PIR is an intrinsic property of many central nervous system neurons and in some cases it results in a burst of action potentials that follows directly after a purely inhibitory synaptic input. Because of this, it has been suggested that PIR may contribute to the maintenance of oscillatory activity in neural networks that are characterized by mutual inhibitory connections, like those involved in locomotor behaviors. In addition, PIR is often included as an element in computational models of neural networks that involve mutual inhibition (Perkel and Maloney, 1974; Perkel, 1976; Roberts *et al.*, 1990). In light of this interest, it is surprising how little is known about the cellular mechanisms responsible for PIR.

Kuffler and Eyzaguirre (1955) concluded that PIR in crayfish stretch receptor neurons is caused by recovery from adaptation during the course of inhibitory hyperpolarization. One feature of that system is that PIR only occurs if the hyperpolarization is imposed on a background of excitation, caused in this case by stretch. They also found that PIR can be elicited in the stretch receptor by hyperpolarizing current pulses. This was an important finding because it showed that PIR is an intrinsic property of

[1] From the Symposium *Swimming in Opisthobranch Mollusks: Contributions to Control of Motor Behavior* presented at the Annual Meeting of the Society for Integrative and Comparative Biology, 4–8 January 2000, at Atlanta, Georgia.

[2] Corresponding author; E-mail: stuartt@leland.stanford.edu

the postsynaptic neuron, related to the membrane potential change associated with inhibition but independent of transmitter receptors or presynaptic properties. The latter conclusion has stood the test of time, marking PIR as a robust property of CNS neurons in a wide variety of contexts (Gerasimov *et al.*, 1966; Hartline and Gassie, 1979; Kandel and Spencer, 1961; Kater, 1974; Selverston *et al.*, 1976; Barrio *et al.*, 1994).

We studied the mechanism of PIR in identified neurons isolated from the buccal ganglia of *Aplysia.* In voltage clamp experiments these cells exhibit slowly decaying inward tail currents after hyperpolarizing voltage steps that have the correct time course and amplitude to explain PIR. A subtraction method was used to isolate slow tail currents for study. The inward tail current after a hyperpolarizing voltage step results primarily from slow recovery of a K^+ conductance from a low level attained during hyperpolarization to a higher level appropriate to the resting potential. The slow K^+ current is voltage dependent and largely insensitive to Ca^{2+} influx. A second process, a non-selective cation current that is activated during more negative voltage steps, also appears to contribute to PIR in some neurons.

METHODS

Specimens of *Aplysia californica* were obtained from Sea Life Supply (Sand City, CA) and kept in flowing sea water at 12–18°C. Buccal ganglia were removed and desheathed and clusters containing B-cells alone or B-cells in combination with A-cells were isolated by undercutting with iridectomy scissors. The normal saline contained (mM); 470 NaCl, 10 KCl, 50 $MgCl_2$, 10 $CaCl_2$, and 5 Hepes, pH 7.5. Ion substitutions appropriate to individual experiments are described in the text or figure legends. The temperature in all experiments was 15°C.

We used standard methods for two microelectrode current clamp and voltage clamp. Voltage electrodes were filled with 3 *M* KCl (10–25 MΩ) while current electrodes were filled with 2 *M* K-D-gluconic acid (30–100 MΩ) to minimize Cl^- loading. Tail currents were low pass filtered at 20 or 80 Hz prior to digitization at a sampling rate of 250 Hz. Iontophoretic injections of Cs^+ and tetraethylammonium (TEA) employed a third pipette and were done under voltage clamp so that the membrane potential did not change during injection. Cs^+ pipettes were filled with 8 *M* CsCl (resistance 5–20 MΩ) or 3.2 *M* $CsSO_4$ (resistance 15–25 MΩ). TEA pipettes were filled with 2.5 *M* TEA.Cl (resistance 40–90 MΩ).

RESULTS

PIR in buccal ganglion B-cells

We studied PIR and its relationship to spike adaptation in neurons B_3 and B_6–B_{10} (B-cells) from the buccal ganglia of *Aplysia californica* using current clamp and voltage clamp methods. In each buccal ganglion there are two identified interneurons, called A-cells by Fiore and Meunier (1979) or B_4 and B_5 by Gardner (1971*a*, *b*), that produce ipsp's in many of the B-cells. A surgical method was used to isolate clusters containing both A-cells and B-cells. This allowed us to examine the response of B-cells to inhibitory synaptic input (Fig. 1A). An individual A-cell was driven to fire a burst of spikes while the hyperpolarization due to summation of ipsp's was recorded in a B-cell. After the stimulus ends the B-cell responds with a postinhibitory rebound that lasts more than a minute (Fig. 1B). It is evident from this experiment that B-cells respond to the cessation of synaptic inhibition with a long lasting period of increased excitability and that this response does not involve excitatory synaptic drive from other sources.

Direct hyperpolarization is followed by PIR in fully isolated B-cells. Six examples are shown in Figure 1C. Each cell exhibits a prolonged increase in firing frequency after the end of a hyperpolarizing current pulse. Some cells begin to fire immediately after the pulse while others begin to fire after a delay that is due to activation of I_A (Connor and Stevens, 1971). All of the initially silent neurons in Figure 1C had rest potentials within 5 mV of −40 mV. Neu-

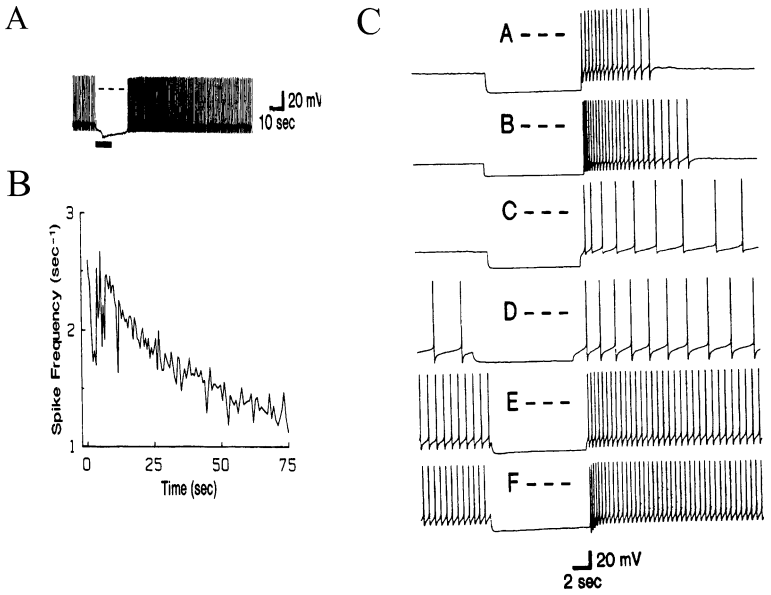

FIG. 1. PIR in isolated B-cells. **A).** Following synaptic inhibition. Intracellular recording from a B-cell in a cluster consisting of B-cells and the two A-cells. An A-cell, impaled with a second microelectrode, was depolarized to fire a burst of spikes for the period indicated by the bar. Dashed line indicates 0 mV. The most negative membrane potential during synaptic inhibition was −50 mV. **B).** Graph of firing frequency as a function of time during PIR. **C).** PIR in fully isolated B-cells following 10 sec hyperpolarizing current pulses. The six examples illustrate the range of response amplitudes and durations seen in this study. Dashed lines indicate 0 mV. Stimulating currents (nA); A) −1.0, B) −5.5, C) −1.6, D) −0.5, E) −0.7, F) −1.2.

rons with rest potentials more negative than approximately −50 mV did not exhibit PIR.

The strength of PIR depends on the amplitude and duration of the preceding hyperpolarization (Fig. 2). Hyperpolarizing pulses of 1 sec or less usually evoke only a single action potential in a fashion similar to anode-break excitation, a property predicted by the Hodgkin and Huxley model. Increasing pulse durations result in PIR responses with greater maximum firing frequencies and longer decay times (Fig. 2C, D). In addition to PIR, B-cells exhibit spike frequency adaptation during maintained depolarization (Fig. 3). The time course of spike frequency adaptation and the decay of PIR are remarkably similar which suggests that PIR and adaptation may be manifestations of a single underlying mechanism.

Voltage clamp studies

In these experiments we are interested in small changes in membrane current in a voltage range close to either the resting potential or the mean interspike voltage in a firing cell. The holding voltage (V_h), therefore, is set near the resting potential (the voltage where $I_m = 0$) and membrane currents are recorded in response to voltage pulses to between −80 and −20 mV. This is the integrative voltage range, the range between the K^+ equilibrium potential and spike threshold. On return to V_h after such a step, one observes a tail current that decays back to the steady level of holding current at V_h (Fig. 4A). These slow tail currents are indicative of the mechanism responsible for both PIR and adaptation. Their slow kinetics, and the voltage range in which they operate set them apart from the much faster conductance changes responsible for action potentials.

We used a subtraction method to isolate slow tail currents for study. Tail currents following 1 sec conditioning pulses were subtracted from the tail currents measured after longer pulses to the same voltage. The difference tail current represents the current component that is activated in the interval between 1 sec and the duration of the lon-

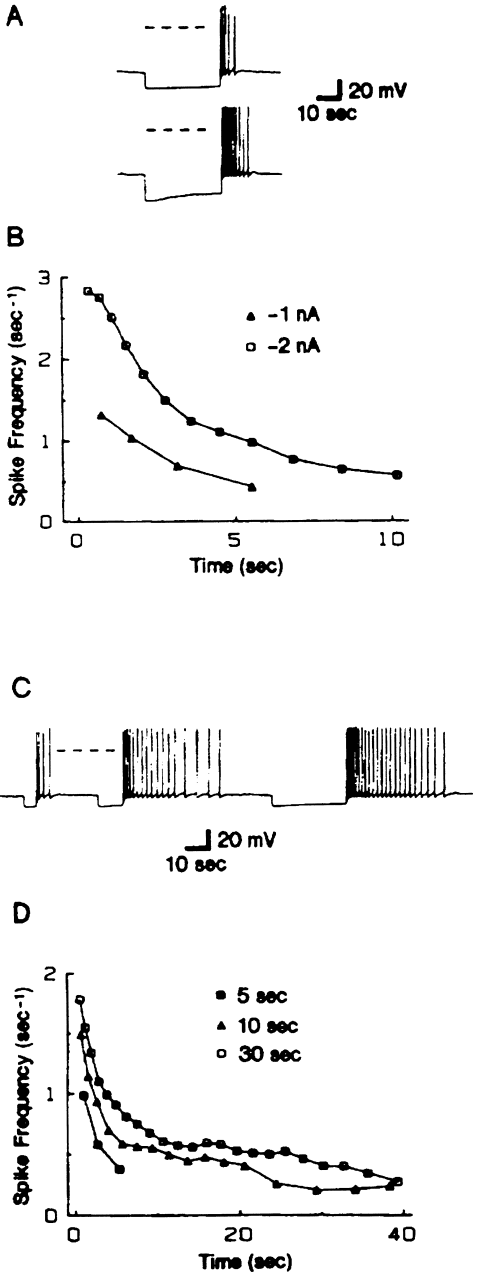

FIG. 2. Sensitivity of PIR to the amplitude and duration of hyperpolarizing current pulses. **A).** PIR in response to 30 sec current pulses, −1 and −2 nA in amplitude (resting potential = −44 mV, zero voltage indicated by dashed line). The maximum voltage during hyperpolarization was −60 mV for the top record and −70 mV for the bottom one. **B).** Graph of firing frequency as a function of time after the hyperpolarizing current steps. **C).** PIR in response to −0.8 nA pulses lasting 1, 5, 10, and 30 sec (resting potential = −45 mV, initial hyperpolarization reached −56 mV). **D).** Graph of firing frequency as a function time.

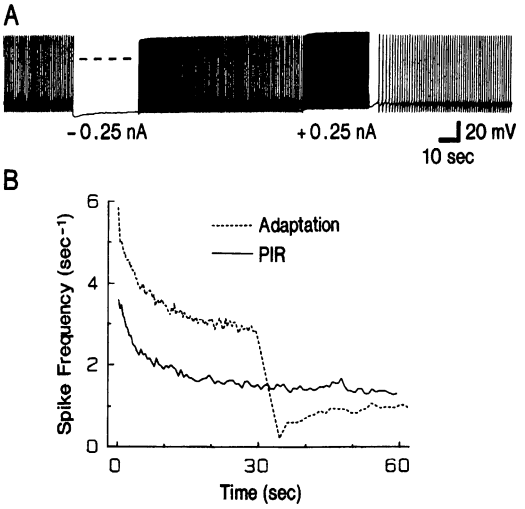

FIG. 3. PIR, spike adaptation, and poststimulus hyperpolarization in an isolated B-cell. **A).** Responses to 30 sec, 0.25 nA hyperpolarizing and depolarizing current pulses (dashed line indicates 0 mV; initial membrane potential during the hyperpolarization = −58 mV). **B).** Graph of firing frequency during PIR (solid line) and during adaptation (dashed line). Note poststimulus hyperpolarization after the end of the depolarizing stimulus.

ger pulse. Examples are shown for conditioning pulses to −80 and −20 mV in Figure 4B. This method eliminates contributions from I_A and all of the other rapidly decaying components of tail current.

A series of voltage clamp pulses is applied to generate families of difference tail currents (Fig. 5A). The amplitudes of difference tail currents are plotted against conditioning potential to obtain a measure of the sensitivity of slow tail current to membrane voltage (Fig. 5B). Depolarizing conditioning pulses activate outward tail currents and hyperpolarizing pulses activate inward tail currents on return to V_h and, therefore, the I(V) curve crosses the zero current axis at the holding potential, −40 mV in this example. The I(V) curves measured in different neurons varied in detail but had several features in common. When tail currents were measured at −40 mV, the slopes of these curves exhibit maxima in the membrane potential ranges between −80 and −60 mV and between −30 and −20 mV. Conditioning pulses in these ranges activate the largest tail currents. The am-

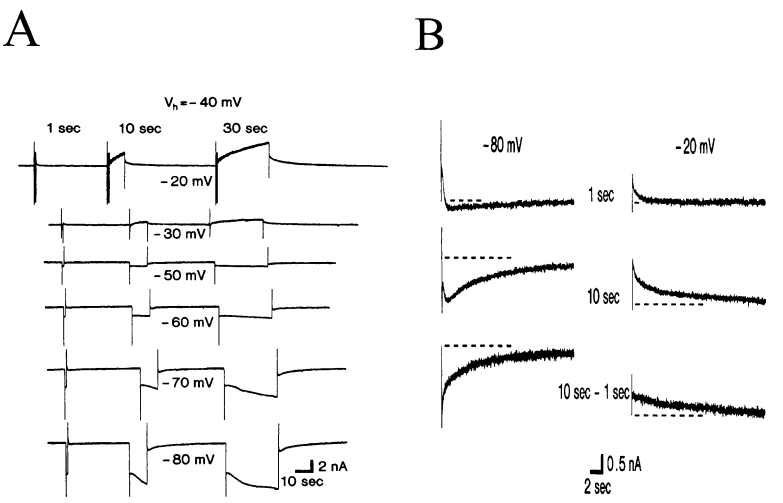

FIG. 4. **A).** Membrane currents during and after 1, 10 and 30 sec steps to a series of voltages from a holding voltage of −40 mV (low pass filter cut-off = 20 Hz). **B).** Subtraction method. Selected tail currents from Part A shown on an expanded scale (dashed lines indicate the holding current preceding pulses). *Top row*: Tail currents after 1 sec conditioning pulses to −80 and −20 mV. *Middle row*: Tail currents after 10 sec pulses. *Bottom row*: The result of subtracting tail currents after 1 sec pulses from tail currents after 10 sec pulses.

plitudes of difference tail currents activated by hyperpolarizations to −50 and −60 mV tend to saturate, so the curves representing 10 and 30 sec pulses converge in that region. On the other hand, the amplitudes of difference tail currents activated by depolarizing conditioning pulses continue to increase as the pulse is lengthened from 10 to 30 sec.

We consistently found that inward tail

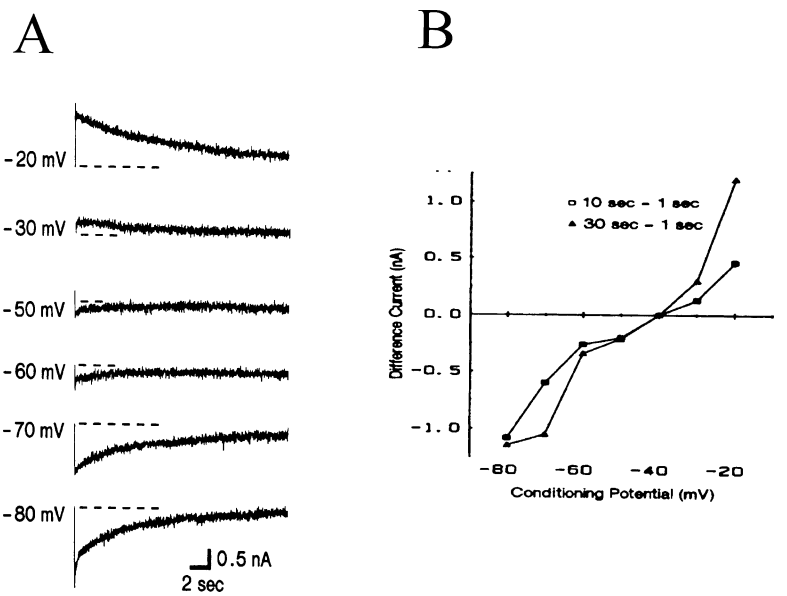

FIG. 5. **A).** Differences tail currents after 30 sec pulses to various conditioning voltages (holding voltage = −40 mV; dashed lines show holding current). **B).** Difference tail current amplitude is plotted as a function of conditioning voltage (amplitudes measured 1 sec after return to holding voltage). *Squares* indicate difference currents after 10 sec pulses. *Diamonds* indicated currents after 30 sec pulses.

currents following hyperpolarizing voltage pulses are very sensitive to the holding potential, V_h. Hyperpolarizing pulses from a holding potential of −60 mV do not result in inward tail currents. Inward tail currents begin to appear at holding potentials near −40 mV and increase in amplitude as the holding potential is made more positive. This finding gave an important clue as to the mechanism responsible for slow tail currents and is addressed again in the Discussion.

The difference method was used to measure the time course of recovery of slow tail currents. The outward tail current after a conditioning pulse to −20 mV falls to one half its initial amplitude ($t_{1/2}$) in 7.2 ± 3.9 sec (mean ± SD, n = 22; range 1.6 to 17 sec) and fully recovers in 44 ± 17 sec (n = 22; range 20 to 78 sec). The value of $t_{1/2}$ for the slow inward tail current after a conditioning pulse to −60 mV was 2.8 ± 3.9 sec (n = 24; range 0.2 to 15 sec) and the current fully recovered in 31 ± 18 sec (n = 24; range 3.4 to 75 sec).

Conductance change and reversal potential

The conductance change and reversal potential of tail currents activated by depolarizing and hyperpolarizing conditioning pulses were measured using a voltage clamp method developed by Johnson (1985). It involves subtracting the instantaneous I(V) relationship measured in control conditions from an instantaneous I(V) relationship measured under experimental conditions to obtain the I(V) relationship of the conductance under study. The slope of the resulting curve indicates whether a conductance increase (positive slope) or decrease (negative slope) is involved and the point where the curve crosses the voltage axis gives the reversal potential of the current.

When an I(V) curve obtained in the absence of a conditioning pulse is subtracted from an I(V) curve obtained during the outward tail current following a depolarizing conditioning pulse, the difference I(V) relationship has positive slope and crosses the voltage axis between −60 and −70 mV (Fig. 6). This indicates that outward tail currents result from a conductance increase to an ion that has a negative equilibrium potential. In contrast, when the control I(V) curve is measured following a 1 sec conditioning pulse to −50 mV and the experimental I(V) curve is measured after a 10 sec hyperpolarization to −50 mV, the difference I(V) curve again reverses near −70 mV but it has a negative slope. This shows that the current activated by the 10 sec hyperpolarization is caused by a conductance decrease.

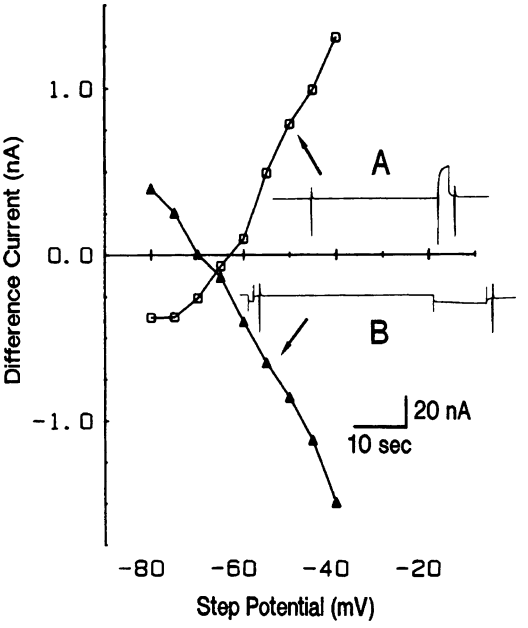

FIG. 6. Instantaneous difference I(V) relationships. Instantaneous currents were measured during a staircase pulse sequence applied during the decay of slow tail currents (measurement periods appear as brief current transients in the inserts). The results are plotted as instantaneous I(V) curves. Each point represents the difference between a control current measurement and an experimental current measurement at the same potential. Insert A shows the procedure for measuring a control I(V) relationship before, and an experimental I(V) relationship after a depolarizing pulse to −20 mV for 2 sec. The difference I(V) relationship is shown by open squares. Insert B shows the method for measuring a control I(V) relationship after a 1 sec hyperpolarizing pulse −50 mV and an experimental I(V) relationship curve after a 10 sec pulse to −50 mV (the staircase pulse sequence was applied 1 sec after return to the holding voltage in both cases). The difference I(V) from the latter experiment is represented by triangles. V_h = −40 mV.

Potassium sensitivity

When the holding potential is −40 mV, depolarizing conditioning pulses are followed by slow outward tail currents and hyperpolarizing conditioning pulses are followed by slow inward tail currents. Hyperpolarizing conditioning pulses also elicit a transient outward current on return to −40 mV due to partial activation of I_A. Each of these tail current components is reversed when the external K^+ concentration is raised from 10 to 100 mM. Assuming an internal K^+ concentration of 250 mM (Sato *et al.*, 1968), the expected value for the K^+ equilibrium potential is −81 mV in 10 mM K^+ and −23 mV in 100 mM K^+ saline. The reversal of tail currents recorded at −40 mV in the presence of 100 mM K^+ shows that these currents are due primarily to changes in K^+ conductance.

The subtraction method was used to isolate slow components of membrane current and construct I(V) curves as before. Figure 7A show that the apparent sensitivity of difference tail currents to increased external potassium depends on the conditioning potential at which the tail currents are activated. The independence relation (Hodgkin and Huxley, 1952) was used to predict changes in the amplitude of a K^+ current resulting from alterations in the K^+ concentration of the bathing saline and the results are plotted as dotted lines in Figure 7A, B. Difference tail currents, measured at −40 mV and activated by conditioning pulses between −60 and −20 mV, are reversed in 100 mM K^+ saline as predicted. However, the difference tail current activated by a conditioning pulse to −70 mV is not reversed and, therefore, exhibits considerably less apparent K^+ sensitivity.

A similar difference in apparent K^+ sensitivity is observed when external K^+ is reduced from 10 to 1 mM (Fig. 7B). Difference tail currents activated at conditioning potentials more positive than −60 mV are increased in low K^+ saline but difference tail currents activated at more negative potentials are decreased. This results in a cross-over in the I(V) curve. It appears that large hyperpolarizations activate a slow current that has a different sensitivity to K^+ than the current activated at less negative potentials and this suggests that a second process in involved.

Intracellular injection of Cs^+, a K^+ channel blocker, markedly reduced difference tail currents activated by depolarizing conditioning pulses and by hyperpolarizing conditioning pulses in the range −40 to −60 (Fig. 7C). This provides additional evidence that the tail current activated in this voltage range is a potassium current. On the other hand, a significant fraction of the tail currents activated by pulses to −70 and −80 mV is resistant to Cs^+, indicating that tail currents activated by pulses to more negative voltages involve some additional process.

TEA was used to further explore the tail currents activated in these two voltage ranges (Fig. 7D). The amplitudes of difference tail currents after conditioning pulses to voltages between −60 and −20 mV are reduced following intracellular injection of TEA. Sensitivity to TEA is observed even in cells that exhibit little change in tail current amplitude following removal of Ca^{2+} from the external medium (Fig. 7D). These data support the conclusion that tail currents activated at voltages positive to −60 mV result primarily from changes in K^+ current and in addition make it unlikely that Ca-dependent-K current contributes significantly to the TEA sensitive component.

Sodium sensitivity

Tail currents are sensitive to replacement (96%) of external Na^+ with N-methyl glucamine (Fig. 8A). The tail currents activated by conditioning pulses more negative than −50 mV are reversed, while tail currents activated by more depolarized conditioning potentials are reduced. Recovery on return to normal saline is greater for the currents activated by large hyperpolarizations than for the K^+ sensitive component activated by more positive conditioning pulses. We can think of two interpretations of this result; either Na^+ contributes to the tail current across all voltage ranges, or the K^+ sensitive component is activated by depolarization from V_h is partially blocked by the application of N-methyl glucamine. When Li^+ was substituted for external Na^+

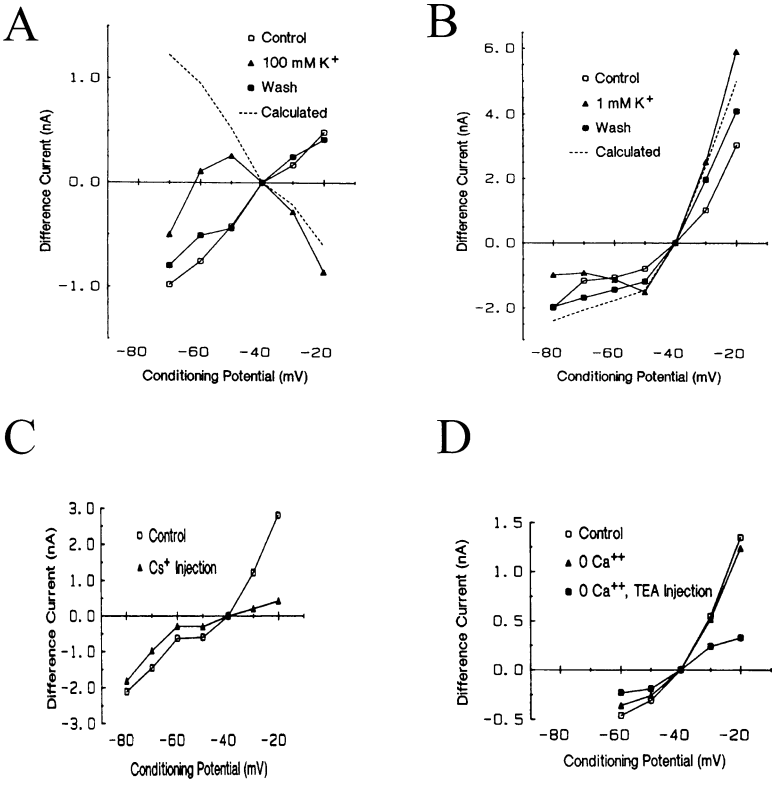

FIG. 7. Sensitivity of difference tail currents to K^+, Cs^+ and TEA. **A).** Effect of increased external K^+ on difference tail currents (obtained by subtracting the tail current after a 1 sec conditioning pulse from the current after a 10 sec pulse; tail current amplitudes measured 0.5 sec after return to −40 mV). *Open squares*: Tail currents in normal saline containing 10 mM K^+. *Triangles*: Currents in 100 K^+ (K^+ replaces Na^+). *Closed squares*: Currents on return to normal saline. The dashed line show the I(V) curve predicted by the independence relation for 100 mM external K^+ assuming a K^+ selective current. **B).** Effect of decreased external K^+ (1 mM K^+; Na^+ replaces K^+; holding voltage = −40 mV). *Open squares*: Difference tail currents in normal saline. *Triangles*: Currents in 1 mM K^+. *Closed squares*: Currents on return to normal saline. *Dashed line*: current predicted from the independence relation. **C).** Effect of intracellular Cs^+ on difference tail currents (obtained by subtracting the current after a 1 sec conditioning pulse from the current after a 30 sec pulse; currents measured 1 sec after return to −40 mV). *Squares*: Tail currents in normal saline before Cs^+ injection. *Triangles*: Currents after iontophoretic injection of $\sim 3 \times 10^{-10}$ mol of Cs^+ from a 100 mM $CsSO_4$ microelectrode. The injection resulted in a greater than 3-fold increase in spike duration (estimated internal Cs^+ concentration: 74 mM for a 200 μm diameter cell and 595 mM for a 100 μm diameter cell assuming a pipette transfer coefficient of 0.5). **D).** Effects of TEA and Ca = free saline on difference tail currents (30 sec conditioning pulses, tails measured 1 sec after return to −40 mV). *Open squares*: Difference tail currents in normal saline. *Triangles*: Currents in Ca-free saline (Mg^{2+} replaces Ca^{2+}, 1 mM EGTA added}. Ca-free saline had little effect on inward or outward tail currents. *Closed squares*: Currents measured in Ca^{2+} free saline after iontophoretic injection of $\sim 0.3 \times 10^{-10}$ moles of TEA (estimated internal TEA concentrations = 6 μM for a 200 micron diameter cell and 48 μM for a 100 micron diameter cell assuming a pipette transfer coefficient of 0.26).

channels, difference tail currents activated by conditioning pulses more negative than −60 mV were reversed but tail currents activated by more depolarizing pulses were little changed (Fig. 8B). Again, it appears that a second current that is sensitive to external Na^+ and Li^+ is activated by strongly negative conditioning pulses.

Calcium sensitivity

The possible contribution of Ca^{2+} influx to difference tail currents was tested by bathing cells in Ca-free saline containing EGTA or by adding the Ca^{2+} channel blockers Co^{2+} or Ni^{2+}. Each of these treatments has been shown to reduce or eliminate the internal Ca^{2+} concentration change

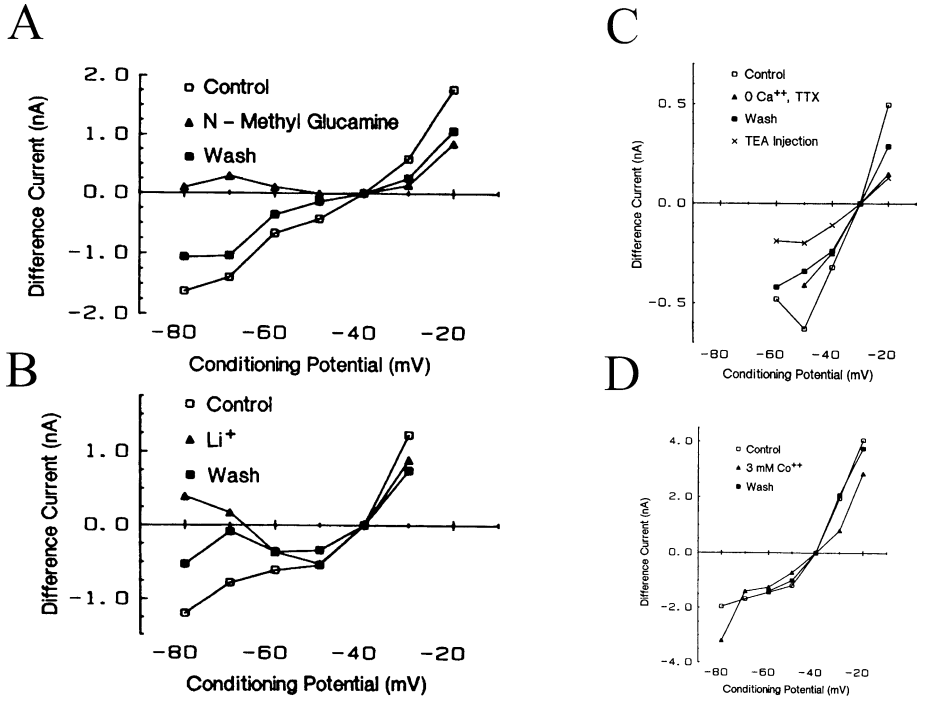

FIG. 8. Effects of external Na^+, Li^+ and Ca^{2+} on tail currents. **A)** *Open squares*: Difference tail currents after 30 sec pulses in normal saline (tail currents measured 0.5 sec after return to −40 mV). *Triangles*: Currents in low Na saline (20 mM NaCl, 450 mM N-methyl glucamine, pH 7.5). *Closed squares*: Currents measured after return to normal saline. **B)** Difference tail currents in Li^+ saline (20 mM NaCl, 450 mM LiCl, pH 7.5). Same procedure as in Part A. *Open squares*: Currents measured in normal saline. *Triangles*: Currents in Li^+ saline. *Closed squares*: Currents on return to normal saline. **C).** Effect of Ca-free saline plus TTX, and TEA injection in the presence of Ca-free saline and TTX. Difference tail currents after 30 sec pulses (currents measured 1 sec after return to −30 mV). *Open squares*: Currents in normal saline. *Triangles*: Currents in Ca-free saline containing 1 mM EGTA and 10 mg/ml TTX. *Closed squares*: Currents on return to normal saline. *X's*: Currents after iontophoretic injection of $\sim 0.5 \times 10^{-10}$ moles of TEA (estimated TEA concentration, 12 μM for a 200 micron diameter cell and 98 μM for a 100 micron cell. **D).** Effect of 3 mM external Co^{2+} on tail currents. Difference tail currents after 10 sec voltage steps (measured 1 sec after return to −40 mV). *Open squares*: Difference tail currents in normal saline. *Triangles*: Currents in 3 mM Co^{2+} saline (3 mM $CoCl_2$ and 7 mM $MgCl_2$ replace all $CaCl_2$). *Closed squares*: Currents on return to normal saline.

responsible for activating the Ca-dependent-K current, I_C (Thompson, 1977). Difference tail currents in the majority of B-cells appear to be only partially dependent on Ca^{2+} influx (Fig. 8C, D) and in some B-cells the tail currents are completely insensitive to Ca-free saline (Fig. 7D).

Chloride sensitivity

When the Cl^- concentration was reduced by replacing two-thirds of external NaCl with Na.gluconate, tail currents activated by conditioning pulses in the range −60 to −20 mV increased (Fig. 9). This was particularly apparent for inward tail currents after hyperpolarizing conditioning pulses. Part of this effect may be due to the positive shift in V_h expected in low Cl^- saline. In addition, a Cl^- conductance has been described in *Aplysia* neurons that appears after the cells have been loaded with Cl^- or exposed to reduced external Cl^- (Chesnoy-Marchais, 1983). This novel Cl^- current could contribute to tail currents measured under the conditions of our experiment since it is activated by hyperpolarizing pulses and has slow kinetics that give rise to slowly decaying tail currents. It is unlikely, however, that the Cl^- conductance that appears under these conditions will contribute to tail currents measured in normal saline. This is because the Cl^- current

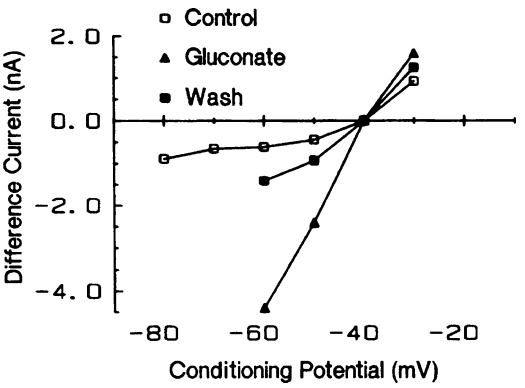

FIG. 9. Effect of decreased external Cl^- on difference tail currents. Difference tail currents were measured after 10 sec conditioning pulses (holding voltage = −40 mV). *Open squares*: Difference currents in normal saline. *Triangles*: Currents in low Cl^- saline (400 mM Na-D-gluconic acid replaces 400 mM NaCl). *Closed squares*: Currents on return to normal saline.

will produce an inward tail only when V_h is more negative than the Cl^- equilibrium potential. Gardner (1971*a*) estimated the reversal potential of the Cl^- dependent IPSP in B-cells to be approximately −75 to −65 mV. In normal saline, therefore, E_{Cl} is more negative than the voltage where we measure tail currents.

DISCUSSION

The inward tail currents we measured are two to three orders of magnitude smaller than the currents that typically occur during an action potential. Nevertheless, they have a strong influence on firing because the resting membrane conductance is so very low. For example in one cell the maximum amplitude of the slow inward tail current at −40 mV was −0.25 nA. In the same cell studied under current clamp, −0.25 nA completely silenced the neuron and +0.25 nA caused a fourfold increase in firing rate.

Our results suggest that at least two different slow ionic currents contribute to the tail currents recorded in B-cells following long lasting voltage clamp pulses in the integrative voltage range. They can be distinguished by their sensitivity to membrane potential, extracellular ion concentrations, and intracellular K^+ current blockers. One current exhibits voltage dependence in the membrane potential range from −60 to −20 mV (and probably to more positive voltages as well), while the other is sensitive to voltage over a more negative, but overlapping membrane potential range from −50 to below −80 mV.

Depolarizing conditioning pulses from the resting potential activate a slow outward current that is associated with an increase in membrane conductance, while hyperpolarizing conditioning pulses to −50 and −60 mV activate a slow inward current that is associated with a decrease in conductance. The reversal potential for both inward and outward tail currents is approximately −70 mV. Both currents are sensitive to changes in external K^+ and both are blocked by intracellular Cs^+ and TEA. All the data suggest that changes in membrane K^+ conductance are involved and the simplest interpretation is that B-cells possess a non-inactivating K^+ conductance that responds slowly to membrane potential changes, that this conductance is minimally activated at −60 mV, and that the conductance increases with depolarization.

The inward current will produce a change in firing frequency only if the current drives the membrane potential beyond threshold. The observation that B-cells rarely exhibit PIR if the resting potential is more negative than about −50 mV can be explained by considering two properties of the inward tail current. First, the small amplitudes of inward tail currents suggest that PIR is most likely to occur if the resting potential is near spike threshold. In addition, the amplitude of the inward current decreases as the holding voltage V_h is made more negative. Thus, more negative resting potentials would be associated with smaller inward currents following hyperpolarization. These two features of the inward tail current are sufficient to explain the resting potential dependence of the PIR responses.

Application of Ca^{2+} free saline and Ca^{2+} current blockers had a minimal effect on tail currents. This indicates that I_C, the Ca-dependent-K current, does not contribute significantly to slow tail currents, at least not at a temperature of 15°C. Tail currents were reduced in some cells by Ca^{2+} channel blockers, but not in the majority of cells and it is clear that a significant fraction of the

slow K^+ current in B-cells is insensitive to changes in Ca^{2+} influx (Thompson *et al.*, 1986).

A Ca^{2+} independent K^+ current with slow kinetics has been described in molluscan neurons that shares a number of properties with the slow K^+ current in B-cells (Thompson *et al.*, 1986; Brodwick and Junge, 1972; Huguenard *et al.*, 1985; Johnson, 1985; Partridge and Stevens, 1976). Two previous studies reported partial reduction in current amplitude following inhibition of Ca^{2+} influx (Huguenard *et al.*, 1985; Johnson, 1985). Interestingly, the activation voltage dependence of the slow K^+ current in *Aplysia* neurons appears to be shifted in the depolarizing direction by approximately 20 mV compared to the current observed in nudibranch neurons (Partridge and Stevens, 1976). We measured a reversal potential of app. −70 which is in the range of published reversal potentials for the slow K^+ current (−77 to −60 mV) estimated from the apparent reversal of the membrane potential response (Brodwick and Junge, 1972), from the apparent reversal of tail currents (Huguenard *et al.*, 1985; Partridge and Stevens, 1976), and from the reversal of subtracted I(V) relationships (Johnson, 1985). It is likely that the potassium current we measured is the same as that described previously.

The large increase in inward tail currents observed when external Cl^- is lowered is difficult to explain. It is possible that reducing Cl^-, or adding gluconate, has a pharmacological effect on the slow K^+ current. However, such an effect would have to be voltage dependent because outward tail currents are much less affected than inward tail currents. Also, Huguenard *et al.* (1985) reported that replacing 90% of external Cl^- with sulfate did not affect the depolarization induced outward tail currents in the neurons they studied. Alternatively, the currents observed in low Cl^- may be contaminated by the Cl^- current described by Chesnoy-Marchais (1983). Whatever the cause, it is not likely that a Cl^- current contributes to PIR under normal circumstances since a Cl^- current will only produce an inward tail current if the Cl^- reversal potential is more positive than the resting potential and this is not normally the case in B-cells.

The slow inward current activated at more negative voltages

The second component of slow current in B-cells is activated by conditioning pulses to more negative potentials. There are two important features of this current to consider. First, because the current is inward at $V_h = -40$ mV, and reverses at that voltage when external Na^+ is reduced, it would seem that Na^+ flux contributes to the current. Johnson (1985) studied a similar current in a different group of *Aplysia* cells and found that it results from a conductance increase and has a reversal potential more positive than 0 mV. This may be a nonselective cation current that is activated by rather strong hyperpolarizations and has slow intrinsic kinetic. The activation curve for this process appears to overlap with the negative end of the integrative voltage range is some cells, so PIR in those cells would result from both recovery from adaptation and the slow decay of an additional inward current. Since the slow inward current is associated with a conductance increase and it has a relatively positive reversal potential, activation of this current by long-lasting inhibition should be self-limiting. This is not the case with the slow K^+ current because it is associated with a decrease in membrane conductance. Thus, IPSPs are not shunted by its activation. Also, hyperpolarization reduces the K^+ driving force so significant inward current development associated with the decrease in K^+ conductance may not be present during inhibition.

The relationship between PIR and adaptation

Our results provide evidence that PIR and spike adaptation are two manifestations of the same process. The decay kinetics of PIR are strikingly similar to the kinetics of adaptation. Neurons that do not adapt lack inward tail currents after conditioning pulses in the integrative voltage range. Both inward and outward slow tail currents are caused primarily by changes in K^+ current; PIR is associated with a decrease in K^+

conductance, while adaptation results from slow activation of a K^+ conductance. The simplest conclusion is that PIR is the result of recovery from tonic adaptation during membrane hyperpolarization. This is consistent with the fact that the slow inward current that underlies PIR is only seen if the holding voltage is more positive than −60 mV. According to our idea, −60 mV must be very near the bottom of the activation curve for the slow K^+ current. Kuffler and Eyzaguirre (1955) reached the same conclusion in their study of slowly adapting stretch receptor neurons in crayfish (see also, Barrio *et al.*, 1994).

Functional role of PIR

The functional importance of PIR is most clearly shown in studies of oscillating neural activity in networks operating primarily through inhibitory synaptic interactions (Anderson *et al.*, 1964; Hartline and Gassie, 1979; Kater, 1974; Satterlie, 1985; Selverston *et al.*, 1983). The idea that emerged from these studies is that PIR provides recurrent excitation in networks of reciprocally inhibitory neurons that acts on a cycle-to-cycle basis to help to maintain oscillation. This idea was successfully demonstrated in modeling studies by Perkel and Malloney (1974) and it has drawn a large number of supporters, too many to list here. PIR has been observed in oscillating neural circuits subserving feeding, locomotion, cardiac function, gastric function, respiration, and singing, with examples drawn from all the major phyletic groups. It is obviously an important property of central neurons that may be involved in a variety of integrative activities. The importance of PIR for network oscillation was perhaps most firmly established in the lobster stomatogastric ganglion. All of the neurons in this ganglion exhibit PIR to some degree (Selverston *et al.*, 1976) and experimental studies combined with a computer model of the network indicate that variability in the temporal characteristics of PIR in different elements contributes to the exact phase relationships observed in the motoneuron output (Hartline and Gassie, 1979).

What is the evidence that PIR provides a source of driving energy that helps to maintaining oscillators in such a network? We propose that PIR results from the removal of tonic adaptation, it is not so much an energy source but rather an energy revealment. The source would have to be tonic excitatory drive that puts the cell into a partially adapted state and we have noted that the cells used in our study and many of the others mentioned in the literature all seem to require a slight depolarization to become tonically adapted before than can express PIR. If the theory holds that PIR is due to a removal of adaptation, then the source of driving energy in many neuronal oscillators remains unknown. In our view PIR and adaptation are present to provide a slow transform, to shape the output of the oscillator into a behaviorally meaningful time frame. The sources of driving energy in a system like this can be anything that shifts the rest potential of key neurons into the adapted state. This might be caused by neuromodulators, internal biochemical events, ionic environment, tonic excitation, etc. In this view, the rest potential of neurons in the core oscillator becomes a sort of switch that can be used to gate oscillation by engaging or disengaging PIR.

ACKNOWLEDGMENTS

We thank the staff of the Hopkins Marine Station for generous support and Dr. Jon Johnson for sharing his expertise and his unpublished data. This study was supported by NSF grant IBN-9514421. The Symposium was supported by National Science Foundation Grant 1BN 990 5990.

REFERENCES

Adams, D. J. and P. W. Gage. 1979. Ionic currents in response to membrane depolarization in an *Aplysia* neurone. J. Physiol. (London) 289:115–141.

Andersen, P., J. C. Eccles, and T. A. Sears. 1964. The ventro-basal complex of the thalamus: Types of cells, their responses and their functional organization. J. Physiol. (London) 174:370–399.

Barrio, L. C., A. Araque, and W. Buno. 1994. Participation of voltage gated conductances on the response succeeding inhibitory synaptic potentials in the crayfish slowly adapting stretch receptor neuron. J. Neurophysiol. Sep; 72(3):140–151.

Brodwick, M. S. and D. Junge. 1972. Post-stimulus hyperpolarization and slow potassium conductance increase in *Aplysia* giant neurone. J. Physiol. London 223:549–570.

Chesnoy-Marchais, D. 1983. Characterization of a

chloride conductance activated by hyperpolarization in *Aplysia* neurones. J. Physiol. London 342: 277–308.

Connor, J. A. and C. F. Stevens. 1971. Voltage clamp studies of a transient outward membrane current in gastropod neural somata. J. Physiol. London 213:21–30.

Fiore, L. and J.-M. Meunier. 1979. Synaptic connections and functional organization in *Aplysia* buccal ganglia. J. Neurobiol. 10:13–29.

Gardner, D. 1971*a*. Bilateral symmetry and interneuronal organization in the buccal ganglia of *Aplysia*. Science 173:550–553.

Gardner, D. 1971*b*. Synaptic organization and bilateral symmetry in the buccal ganglia of *Aplysia*. Ph.D. Diss., New York University, New York.

Gerasimov, V. D., P. G. Kostyuk, and V. A. Maiskii. 1966. Reactions of giant neurons to break of hyperpolarizing current. Fed. Proc. Transl. Suppl. 25:T438–T442.

Hartline, D. K. and D. V. Gassie, Jr. 1979. Pattern generation in the lobster (*Panulirus*) stomatogastric ganglion. I. Pyloric neuron kinetics and synaptic interactions. Biol. Cybern. 33:209–222.

Hodgkin, A. L. and A. F. Huxley. 1952. Currents carried by sodium and potassium ions through the membrane of the giant axon of *Loligo*. J. Physiol. London 116:449–472.

Huguenard, J. R., K. L. Zbicz, D. V. Lewis, G. J. Evans, and W. A. Wilson. 1985. The ionic mechanism of the slow outward current in *Aplysia* neurons. J. Neurophysiol. 54:449–461.

Johnson, J. W. 1985. Membrane conductances of *Aplysia* neurons at voltages near rest. Ph.D. Diss., Stanford University, Palo Alto, California.

Jones, B. R. 1986. Slow ionic currents underlying post-inhibitory rebound in *Aplysia* buccal neurons. Ph.D. Diss., Stanford University, Palo Alto, California.

Kandel, E. R. and W. A. Spencer. 1961. Electrophysiology of hippocampal neurons. II. After-potentials and repetitive firing. J. Neurophysiol. 24: 243–259.

Kater, S. B. 1974. Feeding in *Helisoma trivolvis*: The morphological and physiological bases of a fixed action pattern. Amer. Zool. 14:1017–1036.

Kuffler, S. W. and C. Eyzaguirre. 1955. Synaptic inhibition in an isolated nerve cell. J. Gen. Physiol. 39:155–184.

Partridge, L. D. and C. F. Stevens. 1976. A mechanism for spike frequency adaptation. J. Physiol. London 256:315–332.

Perkel, D. H. and B. M. Mulloney. 1974. Motor pattern production in reciprocally inhibitory neurons exhibiting postinhibitory rebound. Science 185:181–183.

Perkel, D. H. 1976. A computer program for simulating a network of interactingneurons: I. Organization and physiological assumptions. Comput. Biomed. Res. 9:31–43.

Roberts, A. and M. J. Tunstall. 1990. Mutual re-excitation with post-inhibitory rebound: A simulation study on the mechanisms for locomotor rhythm generation in the spinal cord of Xenopus embryos. European J. of Neuroscience 2:11–23.

Sato, M., G. Austin, H. Yai, and J. Maruhashi. 1968. The ionic permeability changes during acetylcholine-induced responses of *Aplysia* ganglion cells. J. Gen. Physiol. 51:321–345.

Satterlie, R. A. 1985. Reciprocal inhibition and postinhibitory rebound produce reverberation in a locomotor pattern generator. Science 229:402–404.

Selverston, A. I., J. P. Miller, and M. Wadepuhl. 1983. Cooperative mechanisms for the production of rhythmic movements. Symp. Soc. Exp. Biol. 37: 55–87.

Selverston, A. I., D. F. Russell, J. P. Miller, and D. G. King. 1976. The stomatogastric nervous system: structure and function of a small neural network. Prog. Neurobiol. 7:215–290.

Thompson, S. H. 1977. Three pharmacologically distinct potassium channels in molluscan neurones. J. Physiol. London 265:465–488.

Thompson, S., J. Smith, and J. Johnson. 1986. Slow outward tail currents in molluscan bursting pacemaker neurons, two components differing in temperature sensitivity. J. of Neuroscience 6(11): 3169–3176.